AFRL-RQ-WP-TP-2014-0193

EXPERIMENTAL INVESTIGATION OF DC-BIAS RELATED CORE LOSSES IN A BOOST INDUCTOR (POSTPRINT)

Hiroyuki Kosai and Zafer Turgut

UES, Inc.

James D. Scofield

Electrical Systems Branch
Power and Control Division

AUGUST 2014

Approved for public release; distribution unlimited.

See additional restrictions described on inside pages

STINFO COPY

AIR FORCE RESEARCH LABORATORY
AEROSPACE SYSTEMS DIRECTORATE
WRIGHT-PATTERSON AIR FORCE BASE, OH 45433-7541
AIR FORCE MATERIEL COMMAND
UNITED STATES AIR FORCE

NOTICE AND SIGNATURE PAGE

AFRL-RQ-WP-TP-2014-0193 HAS BEEN REVIEWED AND IS APPROVED FOR PUBLICATION IN ACCORDANCE WITH ASSIGNED DISTRIBUTION STATEMENT.

*//Signature//	//Signature//
JAMES D. SCOFIELD	GREGORY L. FRONISTA, Chief
Work Unit Manager	Electrical Systems Branch
Electrical Systems Branch	Power and Control Division
Power and Control Division	Aerospace Systems Directorate

REPORT DOCUMENTATION PAGE

Form Approved
OMB No. 0704-0188

1. REPORT DATE *(DD-MM-YY)*	2. REPORT TYPE	3. DATES COVERED *(From - To)*
August 2014	Journal Article Postprint	01 August 2012 – 01 July 2014

4. TITLE AND SUBTITLE
EXPERIMENTAL INVESTIGATION OF DC-BIAS RELATED CORE LOSSES IN A BOOST INDUCTOR (POSTPRINT)

5a. CONTRACT NUMBER
In-house

5b. GRANT NUMBER

5c. PROGRAM ELEMENT NUMBER
62203F

6. AUTHOR(S)
Hiroyuki Kosai and Zafer Turgut (UES, Inc.)
James D. Scofield (AFRL/RQQE)

5d. PROJECT NUMBER
3145

5e. TASK NUMBER
N/A

5f. WORK UNIT NUMBER
Q0M5

7. PERFORMING ORGANIZATION NAME(S) AND ADDRESS(ES)

UES, Inc.
4401 Dayton-Xenia Road
Dayton, OH 45432-1894

Electrical Systems Branch (AFRL/RQQE)
Power and Control Division
Air Force Research Laboratory, Aerospace Systems Directorate
Wright-Patterson Air Force Base, OH 45433-7541
Air Force Materiel Command, United States Air Force

8. PERFORMING ORGANIZATION REPORT NUMBER
AFRL-RQ-WP-TP-2014-0193

9. SPONSORING/MONITORING AGENCY NAME(S) AND ADDRESS(ES)
Air Force Research Laboratory
Aerospace Systems Directorate
Wright-Patterson Air Force Base, OH 45433-7541
Air Force Materiel Command
United States Air Force

10. SPONSORING/MONITORING AGENCY ACRONYM(S)
AFRL/RQQE

11. SPONSORING/MONITORING AGENCY REPORT NUMBER(S)
AFRL-RQ-WP-TP-2014-0193

12. DISTRIBUTION/AVAILABILITY STATEMENT
Approved for public release; distribution unlimited.

13. SUPPLEMENTARY NOTES
PA Case Number: 88ABW-2012-0074; Clearance Date: 06 Jan 2012.

Report published in *IEEE Transactions on Magnetics*, Vol. 49, No. 7, July 2013.

14. ABSTRACT
Soft magnetic components in electronic systems are often subjected to dc bias-flux conditions. These dc bias conditions result in distorted hysteresis loops, increased core losses, and have been shown to be independent of core material. The physical origin of these increased losses is not well understood and there is no simple model that can predict these losses without extensive measurements. Absence of a widely accepted model coupled with the complete lack of dc loss attributes on core manufacturers' data sheets result in a requirement to empirically determine loss values for specific design applications. These deficiencies have motivated our efforts to investigate dc bias dependent loss phenomenon in a Fe-based Metglas core inductor operating in a dc-dc boost converter. Since dc flux levels in the core are proportional to the controllable converter load currents, this topology is ideal to study dc-related losses. Inductor core B-H hysteresis loop characterization was accomplished as a function of switching frequency, input voltage, and load current operating conditions and parameters. In this paper, the core loss results were presented as a function of the dc bias conditions, and the results showed that the core losses increased with the pre-magnetized (Bdc) fields. As a result of our observations, we have proposed a modification to the conventional Steinmetz loss equation to include the effects of dc pre-magnetization flux in the core.

15. SUBJECT TERMS
power electronics, boost converter, interleaved, coupled inductor

16. SECURITY CLASSIFICATION OF: a. REPORT	b. ABSTRACT	c. THIS PAGE	17. LIMITATION OF ABSTRACT:	18. NUMBER OF PAGES	19a. NAME OF RESPONSIBLE PERSON (Monitor)
Unclassified	Unclassified	Unclassified	SAR	10	James D. Scofield
					19b. TELEPHONE NUMBER *(Include Area Code)* N/A

Experimental Investigation of DC-Bias Related Core Losses in a Boost Inductor

Hiroyuki Kosai[1], Zafer Turgut[1], and James Scofield[2]

[1]UES Inc., Dayton, OH 45432 USA
[2]Air Force Research Laboratory, Wright Patterson AFB, OH 45433 USA

Soft magnetic components in electronic systems are often subjected to dc bias-flux conditions. These dc bias conditions result in distorted hysteresis loops, increased core losses, and have been shown to be independent of core material. The physical origin of these increased losses is not well understood and there is no simple model that can predict these losses without extensive measurements. Absence of a widely accepted model coupled with the complete lack of dc loss attributes on core manufacturers' data sheets result in a requirement to empirically determine loss values for specific design applications. These deficiencies have motivated our efforts to investigate dc bias dependent loss phenomenon in a Fe-based Metglas core inductor operating in a dc-dc boost converter. Since dc flux levels in the core are proportional to the controllable converter load currents, this topology is ideal to study dc-related losses. Inductor core $B-H$ hysteresis loop characterization was accomplished as a function of switching frequency, input voltage, and load current operating conditions and parameters. In this paper, the core loss results were presented as a function of the dc bias conditions, and the results showed that the core losses increased with the pre-magnetized $(B_{\rm dc})$ fields. As a result of our observations, we have proposed a modification to the conventional Steinmetz loss equation to include the effects of dc pre-magnetization flux in the core.

***Index Terms*—Hysteresis, inductors, magnetic cores, magnetic losses.**

I. Introduction

OWING to their design requirements or unintentional interference, soft magnetic components in electronic systems are often subjected to dc bias-flux conditions. Inductive elements in switch mode power supplies and core steel sheets in permanent magnet machines are representative of components operating under dc bias-flux conditions. These dc bias conditions result in distorted hysteresis loops and significantly increased core losses, and have been shown to be independent of core material. The physical origin of these increased losses is not well understood. Higher local coercivity and increased hysteresis [1]–[3] and magneto-mechanical damping and/or magnetostriction [4], [5] have been proposed as mechanisms for increased losses under dc bias conditions. Classical theory separating core loss into hysteresis, eddy current, and anomalous components has been insufficient to describe these losses, as have Steinmetz equation predictions [6]. These theoretical deficiencies coupled with the complete lack of dc loss attributes on core manufacturer's data sheets result in a requirement to empirically determine loss values for specific design applications.

These deficiencies have motivated our efforts to investigate dc bias dependent loss phenomenon in a Fe-based Hitachi Metglas core inductor operating in a dc-dc boost converter and an H-bridge system. Since dc flux levels in the core are proportional to the controllable converter load currents, the boost converter topology is ideal to study dc-related losses. Inductor core $B-H$ hysteresis loop characterization was accomplished as a function of switching frequency, input voltage, and load current operating conditions and parameters. In order to compare the hysteresis losses under various dc-bias conditions, peak flux (ΔB) was controlled as a constant at 17 mT through a judicious selection of input voltages and switching frequencies from 50 to 150 kHz. For these experiments, the input voltage/frequency ratio was maintained at 4×10^{-4} V-s, while the load resistance varied in 5 steps (8 Ω, 10 Ω, 13.3 Ω, 20 Ω, and 40 Ω) to achieve the desired dc current variation at each frequency. Temperature dependent data can be enabled through the assembly of the converter, with exception of the low temperature Si CMOS gate control circuit, inside a 200°C capable environmental chamber. Complementary static field magnetic measurements were taken to determine the inductor core's coercivity, saturation magnetization, and permeability. The data is summarized in a discussion of the correlation between the measured static and ac magnetic properties with and without the presence of the dc-bias.

Manuscript received November 02, 2012; revised January 10, 2013; accepted January 16, 2013. Date of current version July 15, 2013. Corresponding author: H. Kosai (e-mail: Hiroyuki.kosai@wpafb.af.mil).

Color versions of one or more of the figures in this paper are available online at http://ieeexplore.ieee.org.

Digital Object Identifier 10.1109/TMAG.2013.2242863

II. Experimental Setup

1) Inductor: An inductor studied for both H-bridge station and dc-dc boost converter experiments was constructed of two pairs of Metglas AMCC 20 C cores [7] without gaps as shown in Fig. 1. The 9:9 E shape inductor has a flux path length of 17 cm and a cross section of 6.6 cm^2. Using an HP4514 LCR meter inductor's self and leakage inductances were measured to be 365 μH and 0.2 μH, respectively.

2) H Bridge System Measurement: A 500 V, 44 A H-bridge inductor test station was built and used to analyze inductor core operating loss characteristics in the absence of pre-magnetization bias field. Fig. 2 shows the schematic of the system for the H-bridge test station unit. Operating frequency and input voltage values, that were identical to the dc-dc converter studies shown in Table I, were selected using an external function generator and a dc power supply. The MOSFETs used for the converter were IXYS IXFT44N50P (500 V, 44 A). The inductor shown in Fig. 1 was used to load the converter in the conventional manner, and the primary current and the secondary voltage were measured and used for the inductor core loss calculations. Converter operation without a dc current

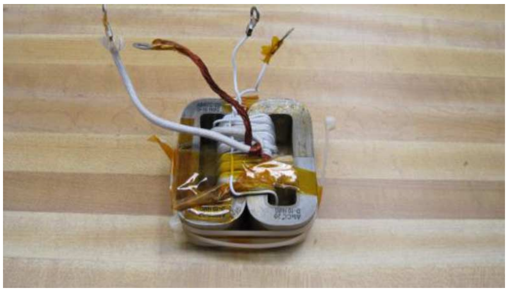

Fig. 1. Experimental inductor built using 2 sets of Metglas AMCC20 C cores. The heavy gauge wires were used for primary and lighter gauge for the secondary winding. Turns ratio was 9:9.

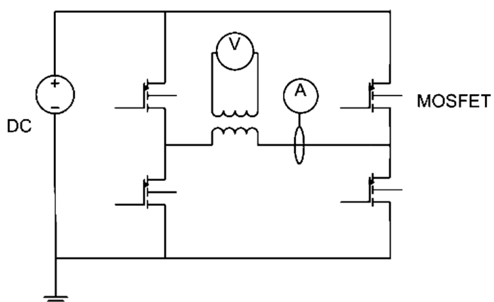

Fig. 2. H-bridge test station system schematic.

TABLE I
DC-DC CONVERTER AND H-BRIDGE OPERATING CONDITION SUMMARY

Applied dc voltage (V)	Inductor frequency (kHz)	ΔB(mT)	Load resistance (Ω)	H_{dc}(A/m)
60	150	16.02	8	1455.9
		16.49	10	1183.2
		16.86	13.3	888.9
		17.05	20	613.6
		17.18	40	318.2
		18.14	NA	0
40	100	16.57	8	982.1
		16.80	10	797.8
		16.78	13.3	603.0
		16.93	20	410.3
		16.97	40	210.7
		17.69	NA	0
20	50	16.37	8	495.5
		16.53	10	397.6
		16.59	13.3	302.8
		16.70	20	204.9
		16.81	40	104.3
		17.85	NA	0

component through the inductor was achieved by utilizing a MOSFET switching duty cycle of 0.5.

3) dc-dc Converter Measurement: In order to generate data consisting of an ac re-magnetization current superimposed on a dc pre-magnetization level in the primary inductor winding, a dc-dc boost converter was used. Fig. 3 shows the schematic of the dc-dc converter that consists of three primary components. Six paralleled SiC diodes (Cree CSD20030) and six SiC JFETs (SemiSouth E120R125) in parallel were used for this experiment to achieve a current rating of 30 A. The same inductor, which was used in the ac-only excitation H-bridge test measurement, was again employed for this evaluation. The output ripple filter consisted of two AVX 300 V, 30 μF capacitors. Since the

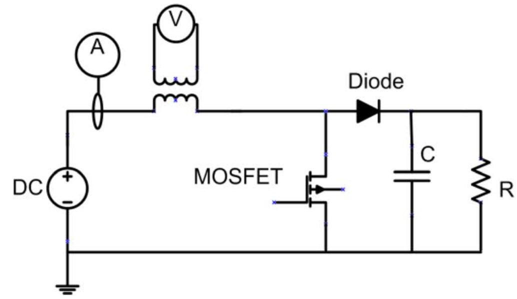

Fig. 3. dc-dc Boost Converter circuit.

experimental setup operated in an environmental test chamber, a 2 m long high temperature coaxial cable was used to access the inductor winding voltage signal. Thus, one end of a 2 m long coaxial cable was connected directly to the secondary winding of the inductor, and the other end of the coaxial cable was connected to an oscilloscope voltage probe (LeCroy PP007). An AP015 LeCroy current probe was used to monitor the primary winding inductor current outside the environmental chamber, which was located 1 m from the inductor.

As a result of these measurement setups, the probe delays due to the cable lengths were characterized and used to adjust the measurement waveforms. For these dc-dc boost converter studies, the JFETs' duty cycle was again chosen to be 0.5. Thus, the magnetic flux density inside the core (B) was determined by the inductor secondary voltage (V), operating frequency (f), primary winding turns (N) and core cross section (A) using Faraday's Law as shown in (1);

$$B = \frac{1}{AN}\int V\,dt + B_{\mathrm{dc}} \tag{1}$$

Further the magnetizing field (H) is a function of inductor primary current (I), number of winding turns, and inductor's average flux path length (L) through Ampere's Law as shown in (2);

$$\oint H dl = IN \tag{2}$$

For the dc-dc converter study, in order to keep the same $\Delta \mathrm{B}_{\mathrm{ac}}$ field during the course of the experiment, input voltage/period ratio was maintained to be constant. To vary H values, load current was varied via resistance selection (8 Ω, 10 Ω, 13.3 Ω, 20 Ω and 40 Ω). Table I summarizes the experimental conditions. All the experimental measurements were recorded using a LeCroy WaveRunner 104MXi.

4) Signal Delay: Since the inductor power loss measurements are very sensitive to the phase shift between secondary voltage and primary current signals, a measurement system error correction was performed. Impedance temporal effects due to the coaxial cable lengths with voltage and current probes, spatially located away from the inductor, results in external delays for which compensation must be included. In order to remove these measurement system delays, the probe signals were calibrated using a low inductance 5 Ω resistor (Multicomp MCTR100T1-5R00JB).

The calibration resistor's resistance and inductance directly measured by HP4514 LCR meter were 4.83 Ω and 2.28 nH for

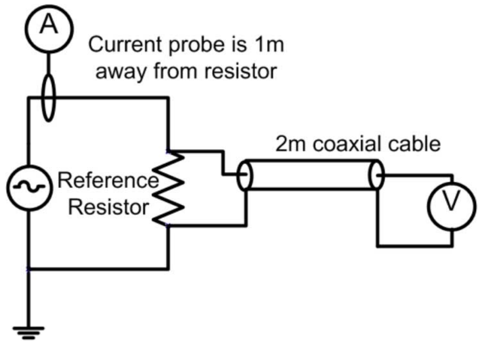

Fig. 4. Experimental time delay calibration setup.

TABLE II
CURRENT SIGNAL DELAY WITH RESPECT TO THE VOLTAGE PROBE SIGNAL FOR THE CALIBRATION SYSTEM

Frequency (kHz)	Scope measurement time resolution (ns)	Current probe time delay wrt Voltage probe (ns)		
		Sine wave	Square pulse	Triangular pulse
50	5	15	~18 (at mid point)	15
100	2	18	~18 (at mid point)	20
150	1	20	~15 (at mid point)	20

all 50, 100 and 150 kHz., and their corresponding time delay and phase shift were 2.28 ns (50, 100 and 150 kHz) and 7.16 E–04 rad (50 kHz), 1.43 E–03 rad (100 kHz) and 2.15 E-03 rad (150 kHz). With the resistor at the inductor position, the same coaxial cables with the function generator, the experimental time delays were measured. Fig. 4 shows the schematic of this time delay calibration system. Square pulses, sine waves, and triangular waves were generated for these calibration studies for various frequencies. The relative time delays between the current probe and the voltage probe and scope's time resolutions were summarized in Table II. It should be noted that the negative delays for 20 kHz results were possibly caused by 10 ns scope time resolution setting. Except for the lower frequency (20 kHz) measurement results, the observed relative delay times between the voltage and current measurement probes was much greater than the scope's temporal resolution and found to be in the 15–20 ns range. When measured waveform data was analyzed, the secondary voltage signals and primary current signals were shifted using these two sets of calibration delays to correct for the hardware induced phase shift.

III. EXPERIMENTAL RESULTS

Fig. 5 shows the B-H curve and permeability for the AMCC20 core material obtained using a B-H analyzer. Since the dc-dc converter measurements only provided relative B field information, static field measurements were necessary to determine absolute B-H curve and permeability information which were used to fit the power loss relations to an expression.

During post data processing, the recorded voltage signal data from the dc-dc converter measurements were shifted to correct for the parasitic cabling impedance shift with respect to the current signal's time. Fig. 6 illustrates the effect on core power loss calculations of a varying I-V phase shift for the 150 kHz 60 V H-bridge waveform signal data. The cable-configuration calibration data for this frequency-voltage product was previously measured to possess a phase shift of 16 ns and is an included data point in Fig. 6 with the remaining points included to illustrate the loss dependence on I-V phase shift.

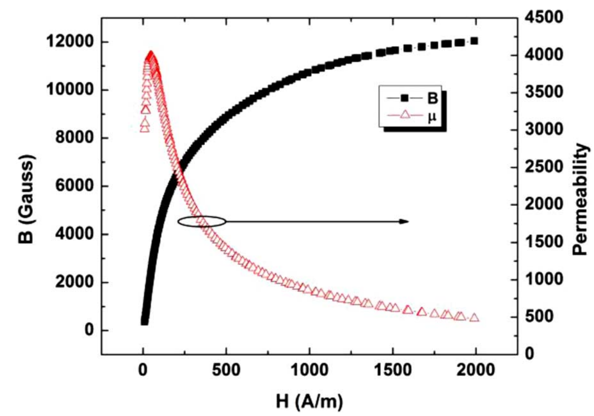

Fig. 5. Measured static magnetic field density, B, and permeability, μ, as a function of magnetic field, H, for the Hitachi Metglas cores.

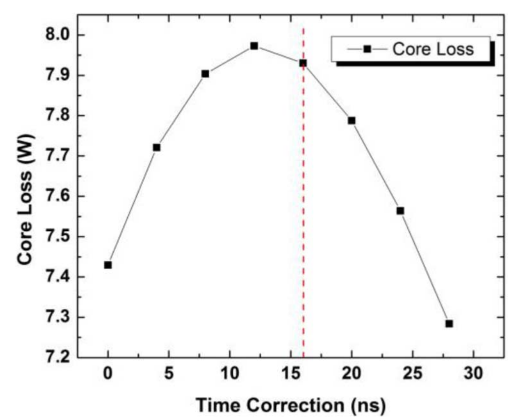

Fig. 6. Core loss (W) was obtained after delaying voltage signals by steps of 4 ns (x-axis in (ns)) with respect to the current signal. The calibrated delay was found to be $\sim$16 ns for this particular data set (150 kHz, 60 V).

IV. DISCUSSION

The Steinmetz equation is given as (3), where P, A, f, and B are power loss density (W/kg), fitting coefficient, frequency (kHz), and flux density (T), respectively.

$$P = Af^{\alpha}B^{\beta} \tag{3}$$

For this particular core material, the manufacturer's data sheet [7] indicates that A, α, and β are 6.5, 1.51, 1.74, respectively. Experimental power loss data with no pre-magnetized $(\mathrm{B_{dc}})$ fields was used to calculate the Steinmetz frequency coefficient. Fig. 7 shows the power losses versus the operating frequency relation while B fields were kept constant. For the experimental data in this figure, the fitted exponential factor, α, was found to be 1.41, rather than the 1.51 value listed in the manufacturers data sheet.

Although these experimental results fit very well with the Steinmetz equation, if there is no pre-magnetization condition in the core, it has been demonstrated[8–11] that the presence of a

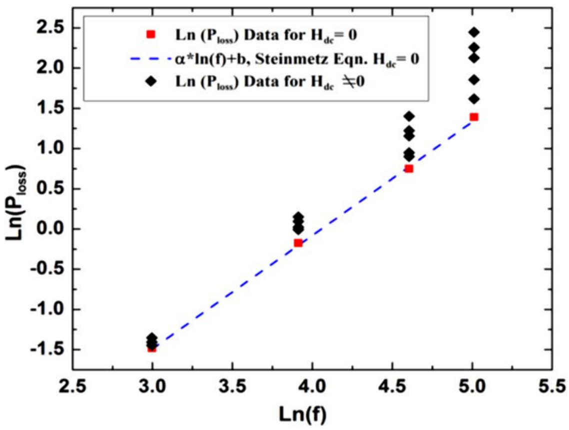

Fig. 7. Experimental core loss values and predicted Steinmetz power loss density curve showing divergence of prediction when $\mathrm{Hdc} \neq 0$.

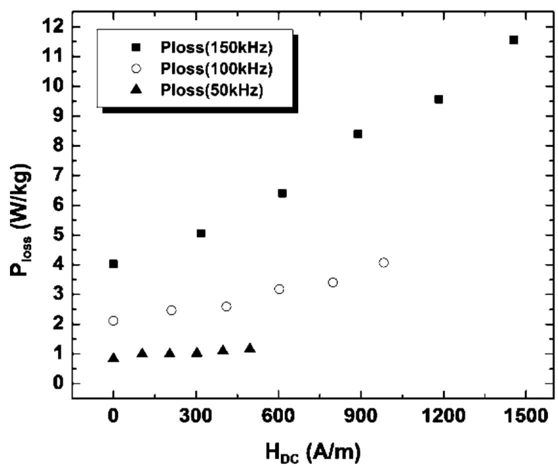

Fig. 8. Power loss density vs. premagnetization fields ($\mathrm{H_{dc}}$ fields) for 150 kHz, 100 kHz, and 50 kHz experimental data.

pre-magnetization field increases core loss values even at identical frequency and $\Delta\mathrm{B_{max}}$ conditions, as seen in Fig. 7 for the $\mathrm{H_{dc}} \neq 0$ data. Furthermore, an exponential increase in the predicted loss error is observed with increasing frequency, which can also be seen in Fig. 7. Fig. 8 shows observed core loss variations with respect to increasing $\mathrm{H_{DC}}$. In order to account for the effect of DC field conditions, we have proposed a modified Steinmetz equation that includes a pre-magnetized field strength factor as shown in (4). It was determined mathematically that an exponential factor with a pre-magnetization field dependent permeability agreed well with the experimental data.

$$P = \frac{A}{\exp(a)} f^{\alpha} B^{\beta} \exp\left[a\left(\frac{\mu}{\mu_0}\right)^{\gamma}\right], \tag{4}$$

where, μ, μ_0, a, and γ are the pre-magnetized permeability, dc permeability, coefficient factor and power factor, respectively. Finally, to obtain correspondence between (3) and (4) when $\mathrm{H_{DC}} = 0$, a normalization condition is achieved by dividing by e^a. Fig. 9 shows experimental power loss points plotted against the predicted power losses of (4). In Fig. 9, γ was chosen to be -1, and fitted parameter, a, was found to be 0.202, 0.172 and 0.141 for 150, 100, and 50 kHz frequency data, respectively.

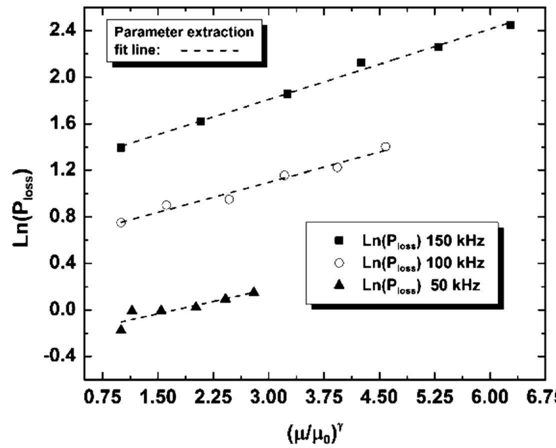

Fig. 9. Ln (Power loss density (W/kg) vs. $[((\mu)/(\mu_0))^{\gamma}]$ for 150 kHz, 100 kHz, and 50 kHz experimental data points. A linear fit was used to extract the parameter, a, for each frequency.

V. Conclusion

DC bias dependent loss phenomenon in a Fe-based Metglas core inductor was investigated using a dc-dc boost converter. For this study, $\Delta\mathrm{B}$ was maintained constant while $\mathrm{H_{DC}}$ was varied by changing the converter's load resistance. Results show that a pre-magnetization field increases core losses, and an empirical relationship was suggested and demonstrated to provide a good fit to experimental loss data. It was also shown that classical Steinmetz prediction error increases with frequency under $\mathrm{H_{DC}}$ conditions, and is thus a critical design consideration for components operating $\geq$100 kHz.

References

[1] C. A. Baguley, U. K. Madawala, and B. Carsten, "A new technique for measuring ferrite core loss under DC bias conditions," *IEEE Trans. Magn.*, vol. 44, no. 11, pp. 4127–4130, Nov. 2008.

[2] V. C. Valchev, A. P. Van den Bossche, and D. M. Van de Sype, "Ferrite losses of cores with square wave voltage and DC bias," in *IEEE Proc. IECON*, Nov. 2005, pp. 837–841.

[3] P. M. Gradzki and F. C. Lee, "Domain wall resonance and its effect on losses in ferrites," in *IEEE Proc. PESC'91*, Jun. 1991, pp. 627–632.

[4] V. J. Thottuvelil, T. G. Wilson, and H. A. Owen, "Unusual high-frequency behaviour of some amorphous metallic-alloy tape-wound magnetic cores," *IEEE Trans. Magn.*, vol. 20, no. 4, pp. 570–578, Jul. 1984.

[5] C. A. Baguley, U. K. Madawala, and B. Carsten, "Unusual effects measured under DC bias conditions on MnZn ferrite material," *IEEE Trans. Magn.*, vol. 45, no. 9, pp. 3215–3222, Sep. 2009.

[6] J. Muhlethaler, J. Biela, J. W. Kolar, and A. Ecklebe, "Core losses under DC bias condition based on Steinmetz parameters," in *Proc. Int. IEEE Power Electr. Conf.*, 2010, pp. 2430–2437.

[7] Hitachi Metals America Ltd., "POWERLITE inductor cores," [Online]. Available: http://www.hitachimetals.com/product/amorphous/powerliteinductorcores/documents/POWERLITE_C_opt.pdf

[8] A. P. Van den Bossche, V. C. Valchev, D. M. Van de Sype, and L. P. Vandenbossche, "Ferrite losses of cores with square wave voltage and DC bias," *J. Appl. Phys.*, vol. 99, p. 08M908, 2006.

[9] H. Fujimori, H. Yoshimoto, and T. Mitera, "Anomalous eddy current loss and amorphous magnetic materials with low core loss," *J. Appl. Phys.*, vol. 52, no. 3, Mar. 1981.

[10] A. Brockmeyer, "Experimental evaluation of the influence of DC premagnetization on the properties of power electronic ferrites," in *IEEE APEC Conf. Proc.*, San Jose, CA, USA, Mar. 1996.

[11] M. Mu, F. Zheng, Q. Li, and F. C. Lee, "Finite element analysis of inductor core loss under DC bias condition," in *IEEE APEC Conf. Proc.*, Orlando, FL, Feb. 2012.